Journal of Cellular Biochemistry 90:387–396 (2003)

Hepatic Stellate Cell Activation In Vitro: Cell Cycle Arrest at G2/M and Modification of Cell Motility

Fabiana M. da Silva,[1] Eduardo L.M. Guimarães,[1] Ivana Grivicich,[2] Vera Maria T. Trindade,[1] Regina Maria Guaragna,[1] Radovan Borojevic,[3] and Fátima C.R. Guma[1]*

[1]Departamento de Bioquímica, ICBS, Universidade Federal do Rio Grande do Sul, Porto Alegre, RS, Brazil
[2]Universidade Luterana do Brasil, Canoas, RS, Brazil
[3]Departamento de Histologia e Embriologia, ICB and PABCAM, Hospital Universitário Clementino Fraga Filho, Universidade Federal do Rio de Janeiro, Rio de Janeiro, RJ, Brazil

Abstract Hepatic fibrosis is a common response to chronic liver injury and is characterized by increased production of extracellular matrix components, whose major part is produced by hepatic stellate cells activated by inflammatory mediators to proliferate and migrate into the injured regions. GRX cells are a model of hepatic stellate cells characterized as myofibroblasts by morphological and biochemical criteria. We have recently shown that they respond to inflammatory mediators and cytokines present in the concanavalin A-activated spleen cell supernatant (SCS) by quantitative changes in the expression of intermediate filaments. The present study investigated the effects of SCS and TNF-α on the GRX cell proliferation and on the organization of the actin cytoskeleton. SCS and TNF-α diminished the culture cell density, with an increase of cell [^{3}H]thymidine incorporation and of cellular protein content, indicating an arrest in the G2/M phase of the cell cycle, which was reversible 48 h after removal of SCS. This effect was abrogated by dibutiryl-cAMP. Actin cytoskeleton reorganization was observed after 24 h treatment, indicating increased cell motility. Our results suggest that inflammation-dependent activation of stellate cells occurs in ordered interaction and coordination of proinflammatory agents. The increase of cAMP levels activates the conversion of lipocytes into myofibroblasts and increases the number of cells that can participate in repair. Since cAMP retains cells in the G1 phase, cytokines of the TNF-α group are required for cell proliferation inducing the entry into the S phase. The progression through the G2/M checkpoint is mediated again by increased cAMP levels. J. Cell. Biochem. 90: 387–396, 2003. © 2003 Wiley-Liss, Inc.

Key words: hepatic stellate cells; proliferation; cytokines; cell cycle; actin cytoskeleton

Liver tissue injury elicits a reparative response involving production of inflammatory mediators, activation of resident macrophages and lymphocytes, and influx of exogenous inflammatory cells. In response to inflammation, resident connective tissue cells that are in the hepatic parenchyma designated "hepatic stellate cells" are activated and induced to proliferate. These phenomena are a hallmark of liver response to injury, providing increased number of myofibroblasts and intense production of a cicatricial extracellular matrix. Conversely, under non-inflammatory conditions, hepatic stellate cells can be induced to store lipids and express the lipocyte phenotype, serving as a repository for lipid-soluble compounds in the body, such as retinoids and steroids. These two complementary and in large part mutually exclusive functions of hepatic stellate cells are orchestrated by hormones and cytokines that can induce and favor expression of the former or the latter phenotype [Pinzani and Gentilini, 1999].

Studies on the GRX cell line that represents murine hepatic stellate cells have led us to propose that quiescent hepatic stellate cells, which are frequent in new-born mice liver and more scarce in older vitamin-A replete animals, have a typical myofibroblast phenotype similar to other perivascular cells [Guma et al., 2001;

Grant sponsor: Ministry of Science and Technology; Grant sponsor: Rio Grande do Sul State Government; Grant sponsor: UFRGS.

*Correspondence to: Fátima C.R. Guma, Departamento de Bioquímica, ICBS, Universidade Federal do Rio Grande do Sul, Rua Ramiro Barcelos 2600-anexo CEP:90035-003, Porto Alegre, RS, Brazil. E-mail: fguma.voy@terra.com.br.

Received 15 April 2003; Accepted 8 July 2003

DOI 10.1002/jcb.10642

© 2003 Wiley-Liss, Inc.

Mermelstein et al., 2001]. This cell line has been established from hepatic inflammatory fibro-granulomatous reactions, which mobilize and activate the adjacent stellate cells of the liver parenchyma [Borojevic et al., 1985; Bolouk̀hère et al., 1993]. Under standard culture conditions, they express the myofibroblast phenotype with morphological and biochemical aspects of the hepatic parenchymal connective tissue cells whose cytoskeleton contains vimentin, desmin, glial acidic fibrillary protein (GFAP), and α-smooth muscle actin (α-SMA) [Guma et al., 2001]. Extensive cloning analysis has shown that GRX cells display several phenotypes: the slowly growing clones with a quiescent phenotype, the fat-storing ones, and the highly proliferating clones similar to the activated myofibroblasts. The ratio among the different clone types was maintained after repeated selective recloning, indicating that the relative distribution of different clones was regulated by an intrinsic mechanism [Monteiro et al., 1995]. GRX cells can be induced in vitro to express the lipocyte phenotype by retinoids or by high levels of insulin, with an overall increase of lipid storage [Margis and Borojevic, 1989; Borojevic et al., 1990; Guaragna et al., 1991, 1992]. Under such conditions, they decrease the proliferation. Conversely, they can reduce the lipid content in presence of compounds that increase cAMP such as caffeine or theophylline (Borojevic, unpublished data). GRX cells are responsive to pro-fibrogenic cytokines, and TGFβ was shown to induce an increase of collagen production [Chiarini et al., 1994], whilst the induction of the lipocyte phenotype is associated with a decreased production of extracellular matrix [Margis et al., 1992; Pinheiro-Margis et al., 1992].

Hepatic fibrosis is associated with chronic inflammation containing cell infiltrates with activated lymphocytes, such as fibro-granulomatous reaction to schistosomal infection or repeated peritoneal injection of xenogenic serum. Inflammatory mediators are expected to elicit both connective tissue cell proliferation and their migration either towards the source of inflammation such as granulomas in the former model [Bolouk̀hère et al., 1993; Lazou et al., 1993], or bridging the major tissue sources of connective tissue cells in perivascular areas, such as formation of dissecting septa in the latter experimental model [Bhunchet and Wake, 1992].

In the present study, we have addressed the question of the effect of lymphokines on the two parameters that are modified in activated hepatic stellate cells during establishment of liver fibrosis: the increase of their number through enhanced proliferation or decreased apoptosis, and cell movement observed in migration of activated cells towards the source of inflammatory agents and formation of fibrotic granulomas or septa. We have used the in vitro model of GRX cells, treated with the supernatant of concavalin-A-stimulated spleen cells, rich in pro-inflammatory cytokines, and with the tumor necrosis factor alpha (TNF-α that has been recognized as one of the major mediators of liver reaction to injury [Britton and Bacon, 1999]. Since both elicited an arrest at the G2/M checkpoint of the cell cycle resulting in an overall decrease of cell density, we also monitored the effect of increased cellular cAMP content, known to occur as a response to other pro-inflammatory mediators. This treatment was required and sufficient to override the G2/M arrest, resulting in the efficient stellate cell proliferation.

MATERIALS AND METHODS

Cell Cultures

GRX, C_2C_{12}, and 3T3 cell lines were obtained from the Rio de Janeiro Cell Bank (PABCAM, Federal University, Rio de Janeiro, Brazil). For the proliferation studies, 10^4 cells/well were seeded into 24-well culture plates; for the flow cytometry analysis, we seeded 5×10^5 cells/25 cm^2 culture flask (Nunc, Roskilde, Denmark). Cells were maintained in Dulbecco's medium (DMEM) with 2 g/l HEPES buffer (both from Sigma Chemical Company, St. Louis, MO), supplemented with 5% fetal bovine serum (FBS) (Cultilab, Campinas, SP, Brazil), pH 7.4, in a humidified atmosphere with 5% CO_2. In different experimental series, the medium was substituted 2 h after seeding by DMEM/FBS containing 2, 5, or 10% spleen cell supernatant (SCS), 50–100 U/ml murine TNF-α, or 0.4 mM dibutiryl cAMP (both from Sigma).

Spleen Cell Supernatant

The SCS was prepared as described by Neuner et al. [1994]. Briefly, murine spleens were mechanically dissociated and homogenized with a Pasteur pipette. The debris was sedimented on ice, the supernatant was

centrifuged, the cells resuspended in Gey's solution, and incubated on ice for 5 min. The cells were harvested, washed, quantified, and seeded 2×10^6 cells/ml. They were incubated for 48 h in a medium containing concanavalin-A (Sigma; 5 µg/ml). Cell cultures were centrifuged and the supernatant was harvested, filtered, and stored at −20°C.

Quantification of Attached Cells by Coomassie Blue

Cells were quantified after 1, 3, and 5 days of culture as described by Margis and Borojevic [1989] with small modifications. Cells that attached to culture dishes after 2 h were considered as T0. The cells were fixed with 4% paraformaldehyde in phosphate-buffered saline (PBS), and stained with 0.2% Coomassie Blue R-250 in 10% (v/v) acetic acid and 40% (v/v) methanol. Subsequently, cells were washed to remove the unbound dye, dried at room temperature, and the adsorbed stain was eluted with 1% SDS (37°C, overnight). The eluted dye was quantified by spectrophotometry at 600 nm. Standard curves were prepared concomitantly by plating cells in densities increasing from 10^4 to 10^5 cells/well.

[^{3}H]Thymidine Incorporation

We used the method described by Kawada et al. [1996]. Cell cultures (3 or 5 days old) were incubated for 24 h with 2 µCi/ml [methyl-^{3}H]thymidine (ARC, Inc., St. Louis, MO), rinsed with cold PBS, precipitated with cold 10% tricholoacetic acid, washed, and dissolved in 0.1 N NaOH. Protein content was monitored according to Peterson [1979], and the incorporated DNA radioactivity by scintillation counting.

Flow Cytometry Analysis

GRX, C_2C_{12}, and 3T3 cells were harvested by trypsin, washed with cold PBS, fixed in 70% ethanol, and stored at −20°C. On the day of analysis, cells were washed with PBS, treated with DNase-free RNase, and stained with 100 µg/ml propidium iodide as described by Lee et al. [1998]. DNA analysis was done using a FACScan (Becton-Dickinson, San José, CA).

Actin Analysis by TRITC–Phalloidin

Cells grown on coverslips were fixed with 4% paraformaldehyde in PBS for 15 min at room temperature and permeabilized with 0.5% Triton X-100. After washing, cells were reacted with TRITC–phalloidin (3.3 µM, 1:100 dilution in PBS, 20 min). The nuclear dye DAPI (both from Sigma) was used at 0.1 µg/ml in 0.9% NaCl, for 5 min as previously described by Mermelstein et al. [2001]. Coverslips were mounted with Fluorsafe (Calbiochem, San Diego, CA). Photographs were taken on Kodak Ektachrome 400 HC film using a Nikon microscope equipped with epifluorescence, using filter sets selective for rhodamine and the blue-wave channel for DAPI.

Statistical Analysis

Results were expressed as mean values of at least triplicates. Statistical analysis was performed using 2-way ANOVA. For post-hoc testing, the Duncan test has been applied. All analysis was performed with the SPSS statistical package (SPSS, Inc., Chicago, IL).

RESULTS

GRX cells maintained in culture under standard conditions were fibroblast-like, organized in parallel strands and whirls. Like other cells of the smooth muscle cell lineage, GRX cells had low contact inhibition and overgrew after confluence into typical "hills and valleys."

When GRX cell cultures were supplemented with concanavalin-A-stimulated SCS that is rich in pro-inflammatory cytokines, an unexpected inhibitory effect of the overall cell growth was observed. Along the studied period, the cell density decreased to approximately 60% of the control (Fig. 1). A low concentration of cytokines was required for this inhibition, since the maximal inhibitory activity was observed already at 2% SCS concentration (Fig. 1A). In order to check the possible effect of concavalin-A, present in SCS, we monitored its effect in the dilution found in 10% SCS (0.5 µg/ml), and we observed no effect on the cell number (Fig. 1B). Moreover, the supernatant of spleen cells prepared under the same conditions but without stimulation by concavalin-A had no effect on the cell quantity (data not shown). These results are in accordance with the reported studies on TNF-α effect on primary cultures of hepatic stellate cells [Saile et al., 1999; Suzuki et al., 2001].

In order to check whether the decreased cell number was due to SCS effect on cell proliferation or apoptosis, we first monitored the [^{3}H]

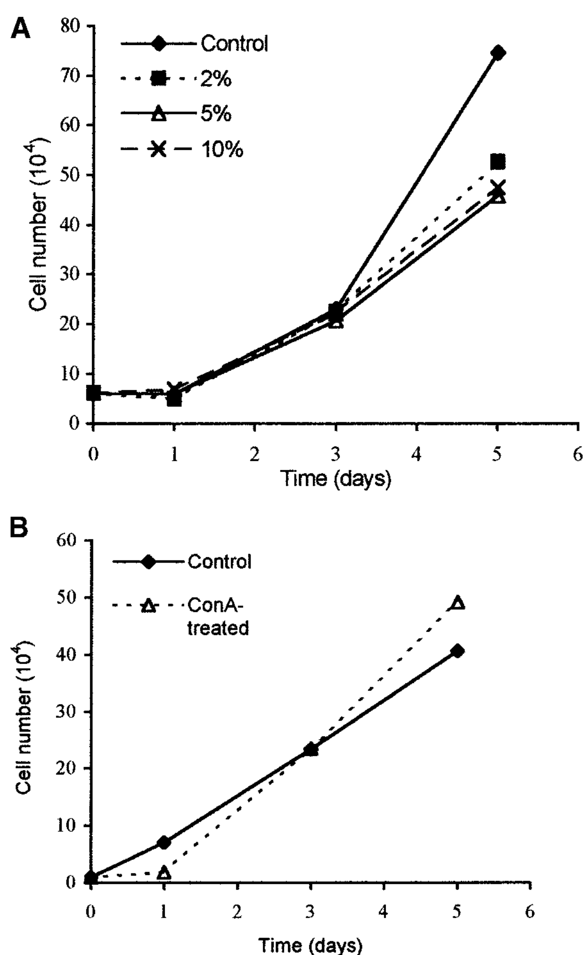

Fig. 1. SCS effect on GRX cell density. **A**: SCS treatment: the cell number at 2, 5, and 10% SCS treatments were significantly reduced on the 5th day of culture, as compared to control ($P < 0.01$). **B**: Concanavalin A treatment: treated cultures were not different from respective controls during the experimental time. The cell number was determined by Comassie Brilliant Blue technique as described at Material and Methods. The results are representative of three experiments performed in triplicate, standard errors (SE) were always 5% lower than their respective means.

thymidine incorporation into GRX cells under the same conditions (Table I). As expected for a lower cell number, the total [^{3}H]thymidine incorporation into SCS-treated cell cultures was significantly reduced. However, the value of cpm/cell was increased in the same cultures as well as the protein content/cell (Table I). These findings raised the question of the cell cycle pattern in SCS-treated cells.

The flow cytometry analysis of DNA showed that the SCS anti-proliferative effect was associated to a G2/M cell cycle arrest. In control and concavalin-supplemented cultures, the cells in G2/M phase were a minor fraction, while in SCS-treated cultures they turned to be the predominant one (Fig. 2A). This effect was specific for hepatic stellate cells, since only a very faint SCS effect was detected on C2C12 myoblast cell line, and no effect was observed on 3T3 cells that have a short G2 phase (Fig. 2B,C, respectively).

It is known that TNF-α is one of the major components of SCS, and its effect on the cell cycle in primary hepatic stellate cell cultures has already been reported [Saile et al., 1999], we monitored whether its effect on the GRX cell cycle was similar to the one observed for SCS. We found that in the two concentrations assayed (50 and 100 U/ml), the 24 h TNF-α treatment had the similar effect on GRX cells, retaining them in the G2/M phase of the cycle. Figure 3 shows results with 50 U/ml TNF-α.

In view of the sensitivity of GRX cells to agents that modify the cell cAMP content, and the fact that an increase of intracellular cAMP can override the G2/M arrest, we questioned whether the apparent decrease of the GRX cell proliferation under the studied conditions could be reverted by modulation of cAMP levels. We observed that the addition of db-cAMP to cultures fully abolished the anti-proliferative effect of TNF-α (Figs. 3 and 4).

In order to monitor whether the SCS-mediated arrest in G2/M phase was reversible, after 4 days of SCS treatment the GRX cells were incubated in the standard medium (Fig. 5). Past 24 h of SCS removal, a decrease at G2/M cells from 38.6% to 21.7% was observed, reaching values close to the controls after 48 h.

TABLE I. [^{3}H] Thymidine Incorporation and Protein Content on GRX Cells

	cpm (per well)	μg protein (per well)	cpm/cell (10^{-3})	μg protein/cell (10^{-4})
Control	4745.2 ± 47.4	97.5 ± 0.47	5.6 ± 0.06	1.15 ± 0.01
SCS	3036.5 ± 105.5[a]	78.8 ± 4.58[a]	6.5 ± 0.21[a]	1.70 ± 0.10[a]

Values represent the mean ± SE of three cultures. The cell number were determined using a Neubauer chamber.
[a]Treated cells are different from controls ($P < 0.02$).

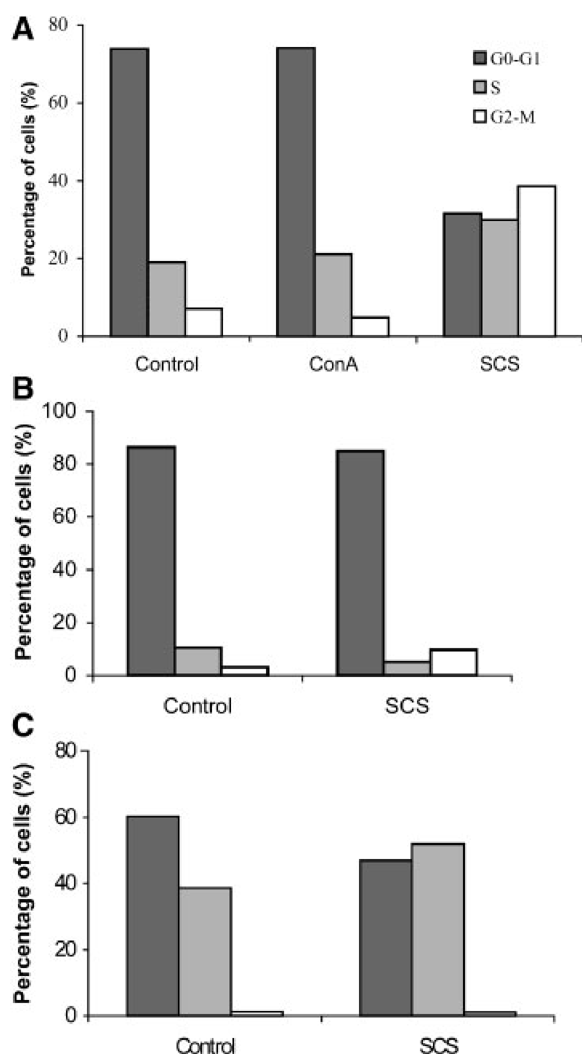

Fig. 2. Cell-cycle analysis of GRX, C2C12, and 3T3 cells after treatment with SCS. **A**: GRX cells: control cells, cells exposed to ConA 0.5 μg/ml, and 2% SCS treated cells; (**B**) C2C12 myoblasts, control cells, and 2% SCS treated cells; (**C**) 3T3 fibroblasts: control cells and 2% SCS treated cells. Cultures were incubated for 5 days with or without 2% SCS. Flow cytometry was evolved as described under Material and Methods. Values given demonstrate percentage subdivision of total culture into distinct cell-cycle phases. The results are representative of three experiments accomplished in the same conditions.

We further monitored the presence of apoptotic cells in the studied model. Under the used conditions, the cell population that contained DNA in quantities below the normal G0/G1 DNA content could not be detected, indicating that only a negligible quantity of cells entered in apoptosis. Accordingly, using the DAPI staining of the nuclei, we detected no apoptotic figures in the studied cultures (not shown).

The morphologic analysis of GRX cells exposed to SCS or TNF-α, and in particular the

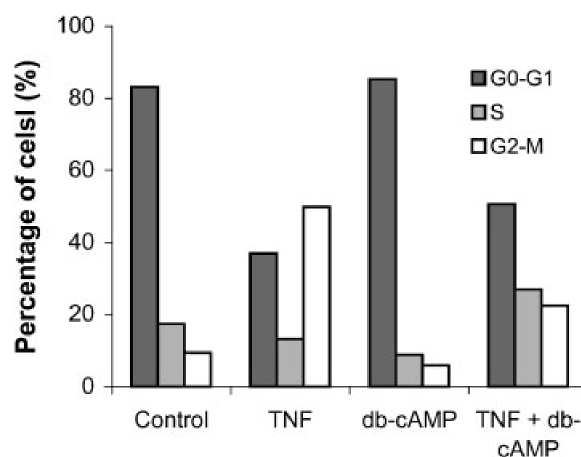

Fig. 3. Cell-cycle analysis on GRX cells: treated with TNF-α and/or db-cAMP. Semi-confluent GRX cells were treated with or without TNF-α (50 U/ml), db-cAMP (0.4 mM), and TNF-α/db-cAMP for 24 h. Flow cytometry was evolved as described under Material and Methods. Values given demonstrate percentage subdivision of total culture into distinct cell-cycle phases. The results are representative of three experiments accomplished in the same conditions.

immunofluorescent staining of actin cytoskeleton, gave two types of information. No signs of cell suffering were observed, in accordance with the full reversibility of the biological effect of the assayed compounds on cell cultures. As previously described [Mermelstein et al., 2001], the control cultures displayed cells with numerous focal adhesions on the substrate and an elaborate system of stress fibers anchored in these well-defined focal adhesions, indicating a stable distribution and organization of cells firmly adherent to the substrate (Fig. 6A). Conversely, both SCS- and TNF-α-treated cells had extensive ruffling membranes with a dense peripheral actin-rich border indicating a frontal cell

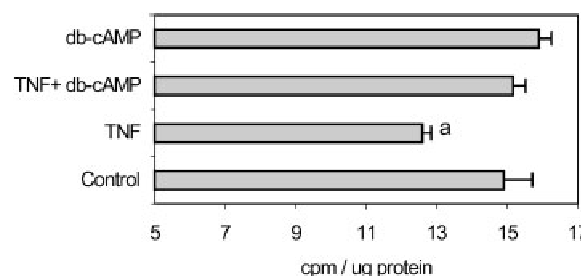

Fig. 4. [^{3}H] Thymidine incorporation on GRX cells treated with TNF-α and/or db-cAMP. Semi-confluent GRX cells were treated with TNF-α (50 U/ml) and or db-cAMP (0.4 mM) for 24 h. [^{3}H] Thymidine incorporation into DNA was assayed at 24 h, as described under Material and Methods. Results are the mean ± SE of four cultures. Shown is a typical experiment repeated twice. a = Treated cells are different from controls ($P < 0.5$).

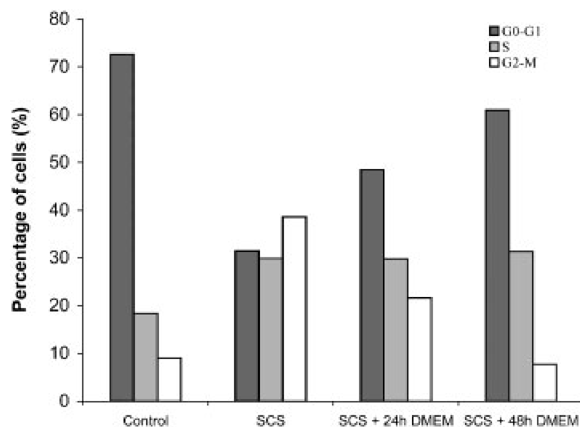

Fig. 5. Reversion of G2/M arrest on GRX cells. Cultures were treated with or without 2% SCS for 5 days and for others 24 or 48 h with free SCS DMEM. Flow cytometry was evolved as described under ''Material and Methods.'' Values given demonstrate percentage subdivision of total culture into distinct cell-cycle phases. The results are representative of three experiments accomplished in the same conditions.

movement, and distant large focal adhesions at the end of long pseudopodia (Figs. 6E and 7C). A proportional decrease of an extensive crossed net of stress fibers was observed. These aspects of cytoskeleton are compatible with an intense cell movement on the substrate. Moreover, small cell clusters were formed (composed of several cells creeping over the others) indicating that the cell–cell adhesion was stronger than the cell–substrate one (Figs. 6C,D and 7A,B).

Taken together, these data indicate that SCS and TNF-α modify simultaneously the cell cycle, the cell movement, and substrate adhesion of GRX cells in culture. The induction of an increase in cell number comparable to that observed in vivo required simultaneously an increase of the intracellular cAMP levels.

DISCUSSION

The present study has shown that GRX cells respond in a complex manner to activation mediated by inflammatory factors present in supernatants of concanavalin-A-stimulated SCS. A similar effect was observed in cultures treated with TNF-α only. These treatments modified the cell cycle causing a strong but reversible arrest in the G2/M phase, and altered their adhesion onto the substrate, as shown by a modification of their focal adhesions and actin cytoskeleton. The latter modification complements the previously described ones concerning modification of intermediate filaments under the similar experimental conditions [Guma et al., 2001].

Hepatic stellate cells are activated in response to liver injuries promoting tissue repair. This response involves cell mobilization and migration towards the lesion, cell proliferation, and increased production of fibrotic extracellular matrix. Pro-inflammatory cytokines play an important role in liver response to injury, and previous studies have shown that they may present both pro- and/or anti-fibrotic effects in vivo, depending upon their dominant activity and the intracellular signal-transducing pathways [Friedman, 1999]. In the present study, we have dissected the coordination of TNF-α pathway and the action of cytokines that increase the intracellular cAMP levels.

The increased cell motility and, in particular, the tendency to adhere and creep over other cells, are representatives of the movement of these cells in inflamed liver. They proliferate and creep towards the granulomatous inflammatory foci in schistosomiasis, where the source of antigens and lymphocyte populations are concentrated, which become surrounded by concentric layers of activated myofibroblasts [Bolоukhère et al., 1993; Lazou et al., 1993]. During the formation of septa in the serum-induced fibrosis, they glide over pre-existing activated stellate cells dissecting the parenchyma [Bhunchet and Wake, 1992]. The actin rearrangement observed in the present study under the effect of SCS and TNF-α is compatible with this in vivo behavior of stellate cells in liver inflammatory reactions.

In the study of cell proliferation, a decrease of the stellate cell number due to the G2/M arrest was somewhat unexpected. An increase is observed in vivo, in fibrotic reactions dominated by lymphocyte-derived inflammatory agents, such as schistosomal liver fibrosis or hepatic septal fibrosis induced by xenogenic serum. A similar G2/M arrest has been reported in primary cultures of rat hepatic stellate cells. Suzuki et al. [2001] reported an elevated number of cells arrested in G2/M phase in the early "activated" phase of cultures (3–4 days), decreasing later on, as well as in subsequent subcultures. Saile et al. [1999] described that in "quiescent" cultures (2 days) TGF-α or TNF-α led to a significant shift of G1 cells into the G2 phase, whereas a shift to G1 arrest was observed in later "activated" cultures (7 days). The latter

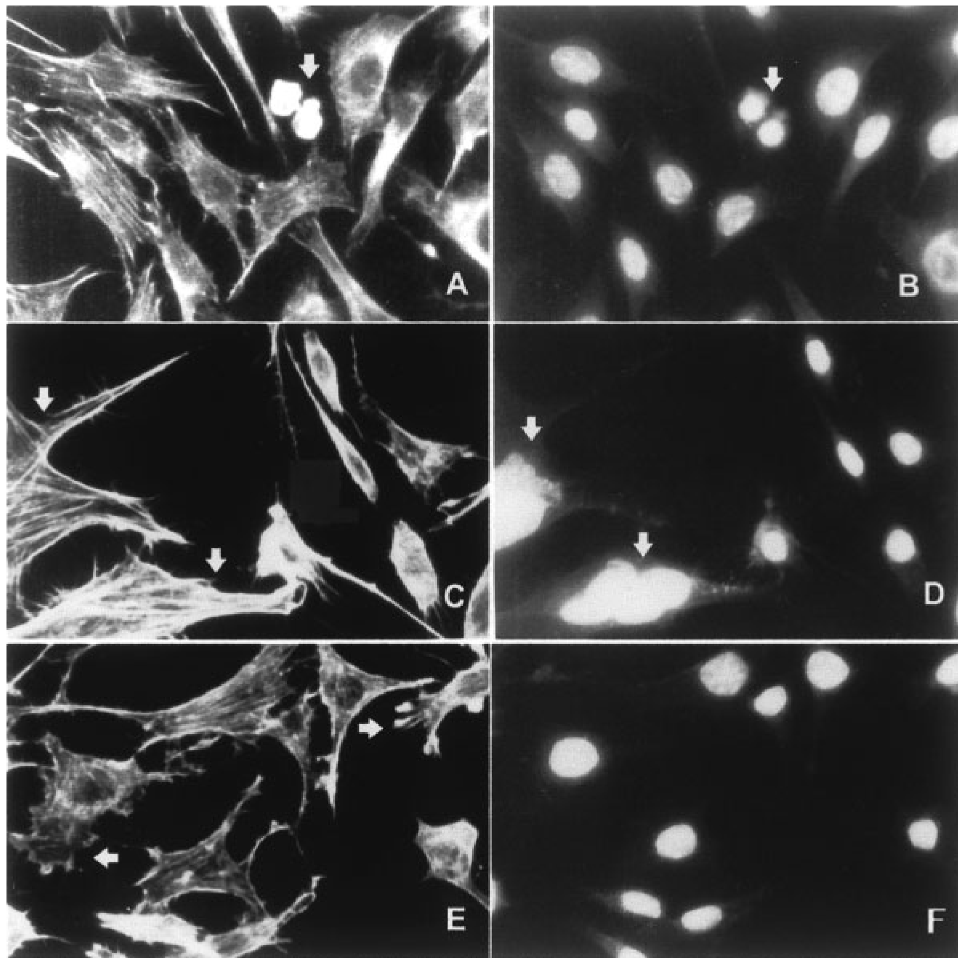

Fig. 6. Effect of 5 days treatment with SCS on actin cytoskeleton. The actin distribution was revealed with TRITC–phalloidin on control (**A**) and on treated cells (**C**,**E**). **B**,**D**,**F**: They show the same cells labeled with the nuclear dye DAPI. At (A) and (B), arrows indicate cells in cytokinesis. At (C) and (D) arrows show several cells creeping over the others. At (E), the arrows indicate the presence of cytoplasmic processes rich on actin, like membrane ruffles. Cells were fixed with 4% paraformaldehyde and permeabilized with 0.5% Triton X-100. Double fluorescence staining was performed as described in Material and Methods. Original magnification 200×.

authors suggested that the arrest in the G2 phase finally resulted in apoptosis. In our hands, no signs of apoptosis were observed in flow cytometry analysis of the cell cycle or in morphological observation of DAPI-stained nuclei, and the observed arrest was fully reversible. The G2/M arrest that leads to apoptosis is characteristic of cell mechanisms that prevent cell replication upon DNA damage, and this is mediated by protective molecular mechanisms such as p53 or BRACA1 [Taylor and Stark, 2001; Yarden et al., 2002]. Since genotoxic effect is not expected to occur under the effect of lymphocyte-derived inflammatory mediators and we have found no signs of apoptosis, the arrest of hepatic stellate cells is potentially dependent upon other, yet undetermined mechanisms.

Liver is a highly vascularized gland, and inflammatory reactions are frequently associated with blood vessel pathology. This is particularly the case of schistosomal liver disease, in which the major pathogens are parasite's eggs embolized in the portal venous radiculi, and worm secreta and excreta brought into the liver by the portal blood flow [Grimaud and Borojevic, 1986; Boloukhère et al., 1993]. Blood and vessel-derived mediators participate in conjunction with lymphokines in induction of a local inflammatory reaction. PDGF-BB, thrombin, and endothelin-1 are examples of cytokines whose effect on hepatic stellate cells has already been described. While PDGF and thrombin can stimulate stellate cell mitosis, it has also been shown that they can generate second

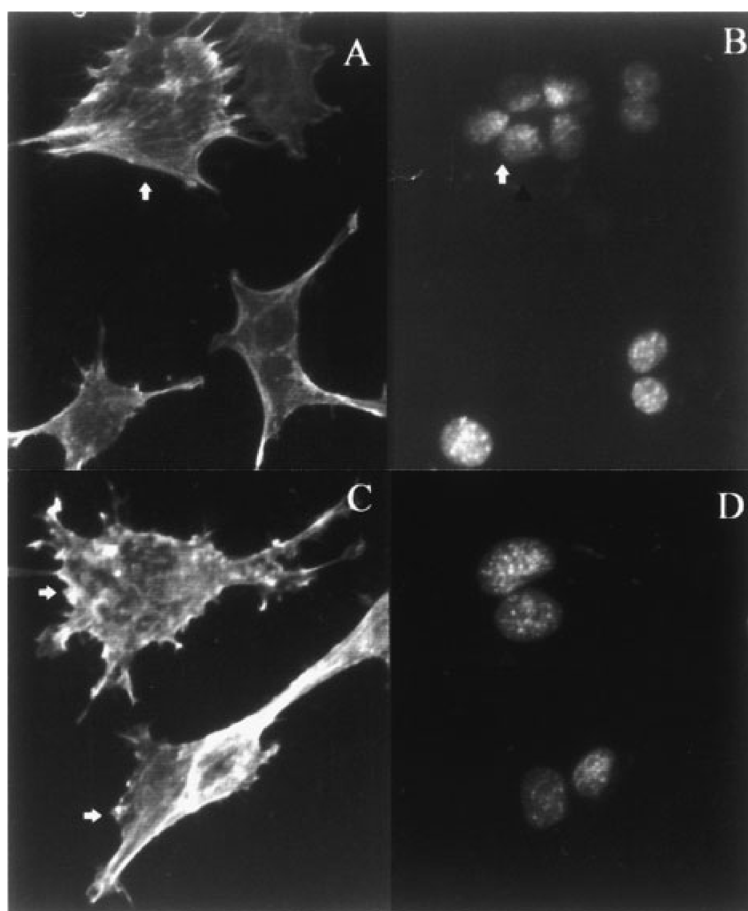

Fig. 7. Effect of 1-day treatment with TNF-α on actin cytoskeleton. **A**,**C**: They show the actin distribution revealed with TRITC–phalloidin. **B**,**D**: They show the same cells labeled with the nuclear dye DAPI. At (A) and (B), arrows show several cells creeping over the others. At (C), arrows indicate the presence of cytoplasmic processes rich on actin, like membrane ruffles. Cells were fixed with 4% paraformaldehyde and permeabilized with 0.5% Triton X-100. Double fluorescence staining was performed as indicated in Material and Methods. Original magnification 200×.

messengers responsible for an inhibitory effect on the same cells. Both cytokines stimulate the synthesis and secretion of prostaglandins (PGE2), which in their turn elevate cAMP production [Mallat et al., 1996, 1998]. While high cAMP levels can decrease phosphorylation of transcription factors involved in cell proliferation, and arrest cells in the G1 phase [Kawada et al., 1999; Kronemann et al., 1999], they can also override the G2/M arrest [Skladanowski, 2002; O'Reilly et al., 2003].

The ordered and coordinated action of the two pathways is apparently required for an efficient supply of cells for tissue repair in liver. The temporary increase of cAMP may be initially required for the decrease of lipid stores in stellate cells expressing the lipocyte phenotype, and their conversion into the reactive myofibroblast phenotype. Since this increase is associated with an arrest in the G1 phase, the activation of the TNF-α pathway elicits the entrance in the S phase, as shown by the increased thymidine incorporation in our model under such treatment. The progression through the G2/M checkpoint requires again the presence of higher cAMP levels, resulting in the overall cycling of the cell population. The finely tuned interplay among inflammatory agents and lymphokines has to be provided for efficient activation of stellate cells and repair of acute liver injury, as well as for the subsequent control of excessive fibrosis in chronic lesions.

Taken together, our studies on GRX cells integrate the homeostasis and the responsiveness of hepatic stellate cells to the local and systemic conditions. The insulin-mediated cAMP controls maintain the expression of the lipocyte phenotype, while the cAMP-increasing compounds reduce the lipid accumulation in GRX lipocytes, converting them to expression of

the myofibroblast phenotype. The associated presence of pro-inflammatory cytokines can further increase the number and activate the myofibroblasts. The cross-talk between cytokines and prostaglandin-cAMP pathways may be mandatory for the reactivity of stellate cells to local injury, as well as to their own proinflammatory potential, known to contribute to controls of liver tissue inflammation [Efsen et al., 2001]. These data are consistent with the proposal that resident quiescent hepatic stellate cells display an undifferentiated phenotype analogous to other perivascular cells of the smooth cell lineages, such as pericapillary pericytes and lung interstitial cells [Guma et al., 2001; Mermelstein et al., 2001]. They can be induced to express alternative phenotypes, activated towards the increased reactivity to inflammatory mediators and increased production of fibrous extracellular matrix, or to accumulation of lipid stores and deposits of lipid-soluble compounds such as retinoids and steroids.

ACKNOWLEDGMENTS

Publication of the Millennium Institute of Tissue Bioengineering. This work was supported by CNPq, FINEP, and PADCT grants of the Ministry of Science and Technology, FAPERGS grant of the Rio Grande do Sul State Government, and PROPESQ grant of the UFRGS.

REFERENCES

Bhunchet E, Wake K. 1992. Role of mesenchymal cell population in porcine serum-induced rat liver fibrosis. Hepatology 16:1452–1473.

Bouloukhère M, Baldo-Correa E, Borojevic R. 1993. Experimental schistosomal mansoni: Characterization of connective tissue cells in hepatic periovular granulomas. J Submicrosc Cytol Pathol 25:505–517.

Borojevic R, Monteiro ANA, Vinhas AS, Domont GB, Mourão PAS, Emonard H, Grimaldi G, Jr., Grimaldi JA. 1985. Establishment of a continuous cell line from fibrotic schistosomal granulomas in mice livers. In Vitro Cell Dev Biol 21:382–390.

Borojevic R, Guaragna RM, Margis R, Dutra HS. 1990. In vitro induction of fat storing phenotype in a liver connective tissue cell line–GRX. In Vitro Cell Dev Biol 25:361–368.

Britton RS, Bacon BR. 1999. Intracellular signaling pathways in stellate cell activation. Alcohol Clin Exp Res 23:922–925.

Chiarini LB, Borojevic R, Monteiro ANA. 1994. In vitro collagen synthesis by liver connective tissue cells isolated from schistosomal granulomas. Braz J Med Biol Res 27:1193–1197.

Efsen E, Bonacchi A, Pastacaldi S, Valente AJ, Wenzel UO, Tosti-Guerra C, Pinzani M, Laffi G, Abboud HE, Gentilini P, Marra F. 2001. Agonist-specific regulation of monocyte chemoattractant protein-1 expression by cyclooxygenase metabolites in hepatic stellate cells. Hepatology 33:713–721.

Friedman SL. 1999. Cytokines and fibrogenesis. Semin Liver Dis 19:129–140.

Grimaud JA, Borojevic R. 1986. Portal fibrosis: Intrahepatic portal vein pathology in chronic human schistosomiasis mansoni. J Submicrosc Cytol 18:783–793.

Guaragna RM, Trugo L, Borojevic R. 1991. Neutral lipid synthesis and accumulation during in vitro induction of the lipocyte phenotype in hepatic connective tissue cells. Biochim Biophys Acta 1085:29–34.

Guaragna RM, Trugo L, Borojevic R. 1992. Phospholipid modifications during conversion of hepatic myofibroblasts into lipocytes (Ito cells). Biochim Biophys Acta 1128:237–243.

Guma FCR, Mello TG, Mermelstein CS, Fortuna VA, Wofchuk ST, Gottfried C, Guaragna RM, Costa ML, Borojevic R. 2001. Intermediate filaments modulation in an in vitro model of the hepatic stellate cell activation or conversion into the lipocyte phenotype. Biochem Cell Biol 79:409–417.

Kawada N, Kuroki T, Kobayashi K, Inoue M, Kaneda K. 1996. Inhibition of myofibroblastic transformation of cultured rat hepatic stellate cells by methylxanthines and dibutyryl cAMP. Digest Dis Sciences 41: 05, 1022–1029.

Kawada N, Ikeda K, Seki S, Kuroki T. 1999. Expression of cyclins D1, D2 and E correlates with proliferation of rat stellate cells in culture. J Hepatol 30:1057–1064.

Kronemann N, Nockher WA, Busse R, Schini-Kerth VB. 1999. Growth-inhibitory effect of cyclic GMP- and AMP-dependent vasodilators on rat vascular smooth muscle cells: Effect on cell cycle and cyclin expression. Br J Pharmacol 126:349–357.

Lazou JM, Zampetti-Bosseler F, Geerts A, Borojevic R, Wisse E. 1993. Tissue distribution of desmin-positive cells in mouse liver during Schisotsoma mansoni infection. In: Wisse E, Knook DL, editors. Cells of the hepatic sinusoid. Vol. 4. Leiden, Holland: Kupffer Cell Foundation. pp 304–307.

Lee JY, Leobhardt LG, Obeid LM. 1998. Cell-cycle-dependent changes in ceramide levels preceding retinoblastoma protein dephosphorylation in G2/M. Biochem J 334:457–461.

Mallat A, Préaux AM, Gal CS, Raufaste D, Gallois C, Brenner DA, Bradham C, Maclouf J, Iourgenko V, Fouassier L, Dhumeaux D, Mavier P, Lotersztajn S. 1996. Growth inhibitory properties of endothelin-1 in activated human hepatic stellate cells: A cyclic adenosine monophosphate-mediated pathway. J Clin Invest 98: 12, 2771–2778.

Mallat A, Gallois C, Tao J, Habib A, Maclouf J, Mavier P, Préaux AM, Lotersztajn S. 1998. Plateled-derived growth factor-BB and thrombin generate positive and negative signals for human hepatic stellate cell proliferation. J Biol Chem 273: 42, 27300–27305.

Margis R, Borojevic R. 1989. Quantification of attached cells in tissue culture plates and on microcarriers. Anal Biochem 181:209–211.

Margis R, Pinheiro-Margis M, Silva LCF, Borojevic R. 1992. Effects of retinol on proliferation, cell adherence

and extracellular matrix synthesis in a liver myofibroblast or lipocyte cell line (GRX). Int J Exp Pathol 73:125–135.

Mermelstein CS, Guma FCR, Mello TG, Fortuna VA, Guaragna RM, Costa ML, Borojevic R. 2001. Industion of the lipocyte phenotype in hepatic stellate cells: Reorganisation of the actin cytoskeleton. Cell Tissue Res 306:75–83.

Monteiro ANA, Geremias AT, Borojevic R. 1995. Clonal heterogeneity in murine liver myofibroblasts. Braz J Med Res 28:457–466.

Neuner P, Klosne G, Schauer E, Pourmojib M, Macheiner W, Grünwald C, Knobler R, Schwarz A, Luger TA, Schwarz T. 1994. Pentoxifylline in vivo down-regulates the release of IL-1β, IL-6, IL-8 and tumor necrosis facto-α by human peripheral blood mononuclear cells. Immunology 83:262–267.

O'Reilly MA, Staversky RJ, Finkelstein JN, Keng PC. 2003. Activation of the G2 cell chekckpoint enhances survival of epithelial cells exposed to hypoxia. Am J Physiol 284L:368–375.

Peterson GL. 1979. Review of the folin phenol protein quantitation method of Lowry. Anal Biochem 100:201–220.

Pinheiro-Margis M, Margis R, Borojevic R. 1992. Collagen synthesis in na established liver connective tissue cell line (GRX) during the induction of the fat-storing phenotype. Exp Mol Pathol 56:108–118.

Pinzani M, Gentilini P. 1999. Biology of hepatic stellate cells and their possible relevance in the pathogenesis of portal hypertension in cirrhosis. Sem Liver Disease 19: 4, 397–410.

Saile B, Matthes N, Knittel T, Ramadori G. 1999. Transforming growth factor beta and tumor necrosis factor alpha inhibit both apoptosis and proliferation of activated rat hepatic stellate cells. Hepatology 30: 1, 196–202.

Skladanowski A. 2002. Modulation of G(2) arrest enhance cell death induced by the antitumor 1-nitroacridine derivative, Nitracrine. Apoptosis 7:347–359.

Suzuki C, Kayano K, Uchida K, Okida K. 2001. Characteristics of cell proliferation profile of activated rat hepatic stellate cells in vitro in contrast to their fibrigenesis activity. J Gastroenterol 36(5):322–329.

Taylor WR, Stark GR. 2001. Regulation of G2/M transition by p53. Oncogene 5:1803–1815.

Yarden RI, Pardo-Reoyo S, Sgagias M, Cowan KH, Brody LC. 2002. BRCA1 regulates the G2/M checkpoint by activating Chk1 kinase upon DNA damage. Nat Genet 30:285–289.